Proton and Lithium Ion Transfer between Two Water Molecules with an External Restraining Force

Tapas Kar and Steve Scheiner*

Contribution from the Department of Chemistry, Southern Illinois University, Carbondale, Illinois 62901

Received August 3, 1994[⊗]

Abstract: Transfer of the central ion in $(H_2O\cdot\cdot H\cdot\cdot OH_2)^+$ and $H_2O\cdot\cdot Li\cdot\cdot OH_2)^+$ is studied by ab initio calculations using the 6-31+G** basis set at the SCF and MP2 levels. An external harmonic force is imposed to restrain the H/Li bond length to the range where two minima exist in the potential energy surface, while providing the two water molecules appropriate flexibility to approach one another during the course of the transfer. The proton transfer barrier is low for a weak external force and climbs as the spring is stiffened. Similar trends are noted as the spring is lengthened with a uniform force constant. The barrier reaches its asymptotic maximum for intermolecular force constants larger than about 7 mdyn/Å, as do the equilibrium and transition state values of R(OO). The energy barrier for Li^+ transfer is somewhat higher than that for proton transfer. The two oxygen atoms more closely approach one another at the midpoint of transfer in either case, and nonlinearity is introduced into the bond as each water molecule pivots around its anchor. The half transfer of the proton involves a displacement of 0.3 Å, as compared to the 1 Å motion of the Li^+. The intrinsic reaction coordinate divides the transfer process into two consecutive steps: The approach of the two O atoms is followed by the actual motion of the central ion. The second step accounts for 70% of the energy required for proton transfer and about 90% in the Li^+ case. Most of the electron density rearrangement takes place in the second step of either transfer.

1. Introduction

Due to its importance in various chemical and biological reactions, the proton transfer process has been an active field of research[1−6] for the last two decades. The simplicity of the $(H_2OH\cdot\cdot OH_2)^+$ complex has permitted it to serve as a prototype for investigating the fundamentals of the proton transfer reaction in larger and more complex systems. However, one difficulty with using $(H_2OH\cdot\cdot OH_2)^+$ as a vehicle to study proton transfer is that its equilibrium geometry contains an extraordinarily short H bond, with R(O··O) ~ 2.4 Å.[7] Such a short interoxygen distance is very rare. In proteins, for example, H bonds are typically in the 2.7−3.2 Å range,[8] due to constraints imposed by the protein on each internal H bond as it adopts its overall three-dimensional structure. As a consequence of its very short H bond, the potential energy surface (PES) of $(H_2O\cdot\cdot H\cdot\cdot OH_2)^+$ contains only one minimum, which places the proton precisely midway betwen the two oxygens. It is hence problematic to consider the transfer of a proton between the two water molecules of $(H_2O\cdot\cdot H\cdot\cdot OH_2)^+$ *per se*.

In order to study proton transfers in the longer H bonds characteristic of macromolecules, computations involving $(H_2O\cdot\cdot H\cdot\cdot OH_2)^+$ have typically not allowed R(O··O) to relax to its very short optimal length. Instead, this distance has been frozen at some arbitrary longer value during the entire course of the proton's displacement. The energetics computed for proton transfer in this way consist of a "slice" through the full PES of $(H_2O\cdot\cdot H\cdot\cdot OH_2)^+$. Calculations over the years have demonstrated[9] that the energy profile along such a slice does in fact contain a pair of minima, separated by a barrier; the height of this barrier rises quickly as R(O··O) is stretched.

Such an approach of fixing the interoxygen separation is not entirely satisfactory for a number of reasons. In the first place, calculations in other systems have shown that there is a tendency for the two subunits of the H bond to approach one another more closely as the proton reaches the midpoint of its transfer. Freezing R(O··O) prevents any such adjustment which might be an important part of the energetics of the system. Moreover, a constant interoxygen distance is not representative of a protein or other large molecule where there are vibrational motions that cause oscillations in the H bond geometry. Indeed, recent work has illustrated the importance of coupling proton transfer energetics to fluctuations in the length of the H bond.[10] From a computational standpoint, an artificial restriction of a fixed intermolecular separation, longer than the equilibrium value, prevents the system from attaining a true minimum in its many-dimensional PES; nor does the midpoint in the transfer represent a genuine first-order stationary point, i.e. a transition state.

One way to address these concerns is to consider how the embedding of a hydrogen bond in a macromolecule affects its behavior. In the context of a protein, the hydroxyl groups that participate in H bonds are typically the terminus of the side chain of a Ser or perhaps Thr residue. Modeling by a water molecule hence consists of replacing the C atom to which the −OH is attached by a hydrogen. The manner in which these atoms attach the H bond to the protein skeleton is depicted as

[⊗] Abstract published in *Advance ACS Abstracts*, January 15, 1995.

(1) Caldin, E. F.; Gold, V. *Proton Transfer Reactions*; Halsted: New York, 1975.
(2) Stewart, R. *The Proton: Applications to Organic Chemistry*; Academic: Orlando, FL, 1985.
(3) Meot-Ner, M.; Smith, S. C. *J. Am. Chem. Soc.* **1991**, *113*, 862.
(4) Firth, D. W.; Beyer, K.; Dvorak, M. A.; Reeve, S. W.; Grushow, A.; Leopold, K. R. *J. Chem. Phys.* **1991**, *94*, 1812.
(5) Dodd, J. A.; Baer, S.; Moylan, C. R.; Brauman, J. I. *J. Am. Chem. Soc.* **1991**, *113*, 5942.
(6) Scheiner, S. *Adv. Biophys. Chem.* **1993**, *3*, 119.
(7) Latajaka, Z.; Scheiner, S. *J. Mol. Struct. (THEOCHEM)* **1991**, *234*, 373 and references cited therein.
(8) Jeffrey, G. A.; Saenger, W. *Hydrogen Bonding in Biological Structure*; Springer-Verlag: Berlin, 1991.
(9) (a) Scheiner, S. *J. Phys. Chem.* **1982**, *86*, 376. (b) Scheiner, S. *J. Am. Chem. Soc.* **1981**, *103*, 315. (c) Scheiner, S.; Bigham, L. D. *J. Chem. Phys.* **1985**, *82*, 3316. (d) Scheiner, S. *Acc. Chem. Res.* **1985**, *18*, 174. Scheiner, S. *Acc. Chem. Res.* **1994**, *27*, 402. (e) Cybulski, S. M.; Scheiner, S. *J. Am. Chem. Soc.* **1989**, *111*, 23.
(10) Chapman, S.; Ali, D. P.; Hynes, J. T. *Chem. Phys.* **1989**, *136*, 297. Timoneda, J. J.; Hynes, J. T. *J. Phys. Chem.* **1991**, *95*, 10431.

0002-7863/95/1517-1344$09.00/0

Chart 1

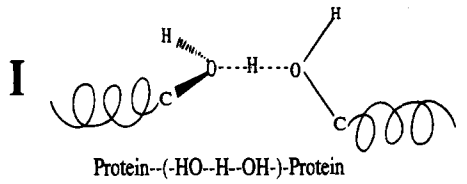

Chart 2

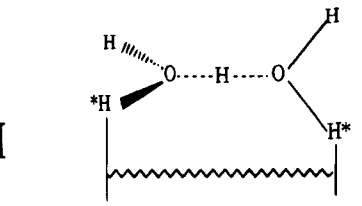

a cartoon in Chart 1, where springs represent the flexible connection to the remainder of the protein. This situation can be modeled by considering one H atom of each water in $(H_2O\cdot\cdot H\cdot\cdot OH_2)^+$ as an "anchor" atom, denoted by an asterisk in chart 2. Rather than fix the two H* atoms at any particular positions, the flexibility of the protein can be simulated by an external force applied to them. Such a force should allow the distance between the two anchor atoms to fluctuate during the course of the proton transfer but at the same time should prevent them from approaching so closely as to yield a H bond shorter than is relevant to proteins. This sort of approach permits not only fluctuations in the distance between the molecules via "pulling" against the external potential but also pivoting around the H* atoms, allowing the two oxygens to approach one another while leaving the anchors unmoved so no force need be exerted against the external potential. Keeping the two water molecules a "respectable" distance from one another not only better represents the situation within a protein but also prevents the collapse of the proton transfer potential function to a single-well potential. It then becomes possible to obtain true minima and transition states on the modified PES.

The merits of this strategy are explored in the present paper. We consider how the external force between the two anchor hydrogens affects the energetics of the proton transfer process and the geometries of the minima and transition states on the modified PES. Also investigated is the sensitivity of the various properties to the magnitude of the external force. In comparison to the reams of data and interpretation that have built up over the years concerning the H bond and proton transfer, the analogous Li bond[11] and lithium ion transfer[12] remain largely unexplored, motivating us to perform analogous calculations on $(H_2O\cdot\cdot Li\cdot\cdot OH_2)^+$ for purposes of comparison. Of particular interest are the differing minimum energy paths for the Li^+ and H^+ transfers and the manner in which electron densities are redistributed along these pathways.

2. Computational Details

All calculations were carried out using the Gaussian 92 code.[13] One hydrogen on each water molecule was chosen as an "anchor" atom and is labeled below as H*. To the quantum mechanical energetics of the system was added an external restraining force in the form of a harmonic potential between the anchored hydrogens

$$V(H^*H^*) = {}^1/_2k[r(H^*H^*) - r_e]^2 \quad (1)$$

The k parameter represents a force constant which is a measure of the stiffness of the restraining force. In the absence of any quantum mechanical intermolecular potential between the two water molecules, the anchor hydrogens would be located a distance of r_e from one another. As a starting point for our calculations, these equilibrium H*H* distances are taken as 4.5 and 7.5 Å in $(H_2O\cdot\cdot H\cdot\cdot OH_2)^+$ and $(H_2O\cdot\cdot Li\cdot\cdot OH_2)^+$, respectively. This choice of r_e leads to $R(O\cdot\cdot O)$ distances in the range 2.7−3.0 Å in the protonated complex and 5.4−5.9 Å in $(H_2O\cdot\cdot Li\cdot\cdot OH_2)^+$, when the full quantum mechanical forces are added. The force constant in eq 1 is varied over a wide range from 0.2 to 20.0 mdyn/Å in order to cover a spectrum of differing flexibility of the protein skeleton.

Calculations are performed at both SCF and MP2 levels. Numerous prior calculations[7,14] have demonstrated that most of the important correlation aspects of the proton transfer process are contained within the second-order Moller−Plesset (MP2) level. Full geometry optimizations were carried out with no symmetry constraints. The basis set used in the present study is of split valence (6-31G) type with polarization functions added to all the atoms and a set of diffuse functions on O and Li. Diffuse functions on H have been seen to have a negligible effect on the H bond energies[15] and are hence not included in the basis set. Single-point calculations are performed at the SCF, MP2, MP3, and MP4SDTQ levels for the SCF and MP2-optimized geometries to be sure that correlation has been properly accounted for. Zero-point vibrational energies have been evaluated at both SCF and MP2 levels and then added to electronic energies to obtain the vibrationally adiabatic potential. Scale factors recommended by Pople et al.,[16] 0.9135 and 0.9646 for SCF and MP2 levels, respectively, have been used to correct these vibrational energies.

Fukui[17] has formulated a so-called intrinsic reaction coordinate (IRC) method by which it is possible to trace a steepest descent path from the transition state toward reactants and products. The IRC path generated in this way provides energy profiles for chemical reactions. In order to obtain further insight into the H^+ and Li^+ transfer reactions, IRC calculations[18] were performed at the SCF level. The IRC pathway was computed in mass-weighted internal coordinates with a stepsize of 0.4 $amu^{1/2}$ bohr. No symmetry constraints were employed in the IRC calculations.

3. Results and Discussion

1. Structure and Geometries. The equilibrium and transition state geometries of the two complexes are exhibited in Figure 1, along with the atomic numbering scheme. Details of the geometries, fully optimized at both SCF and MP2 levels, are listed in Tables 1 and 2 for a given set of parameters k and r_e in the external potential. It might first be observed that the H bonds are significantly distorted from linearity in each case. For example, the θ(O2O1H3) angle is 18° in the MP2 optimized $(H_2O\cdot\cdot H\cdot\cdot OH_2)^+$ equilibrium complex. This nonlinear distortion arises when the attractive intermolecular force pulls the oxygens together by pivoting around the anchor hydrogens. (It is this same sort of external force that is responsible for the nonlinear character of most H bonds within protein molecules.) The attraction between the oxygen atoms apparently grows stronger as the proton reaches the O··O midpoint, as evidenced by (a) a more nearly linear O··H··O arrangement and (b) a

(11) Sannigrahi, A. B.; Kar, T.; Niyogi, B. G.; Hobza, P.; Schleyer, P. v. R. *Chem. Rev.* **1990**, *90*, 1061.
(12) Duan, X.; Scheiner, S. *J. Phys. Chem.* **1992**, *96*, 7971.
(13) Frisch, M. J.; Trucks, G. W.; Head-Gordon, M.; Gill, P. M. W.; Wong, M. W.; Foresman, J. B.; Johnson, B. G.; Schlegel, H. B.; Robb, M. A.; Replogle, E. S.; Gomperts, R.; Andres, J. L.; Raghavachari, K.; Binkley, J. S.; Gonzalez, C.; Martin, R. L.; Fox, D. J.; DeFrees, D. J.; Backer, J.; Stewart, J. J. P.; Pople, J. A. *Gaussian 92*; Gaussian Inc.: Pittsburgh, PA, 1992.
(14) (a) Szczesniak, M. M.; Scheiner, S. *J. Chem. Phys.* **1982**, *77*, 4586. (b) Del Bene, J. E. *J. Phys. Chem.* **1988**, *92*, 2874. (c) Frisch, M. J.; Del Bene, J. E.; Binkley, J. S.; Schaefer, H. F., III *J. Chem. Phys.* **1986**, *84*, 2279.
(15) Del Bene, J. E. *J. Comp. Chem.* **1987**, *8*, 810.
(16) Pople, J. A.; Scott, A. P.; Wong, M. W.; Radom, L. *Isr. J. Chem.* **1993**, *33*, 345.
(17) Fukui, K. *Acc. Chem. Res.* **1981**, *14*, 363.
(18) Gonzalez, C.; Schlegel, H. B. *J. Phys. Chem.* **1990**, *94*, 5523.

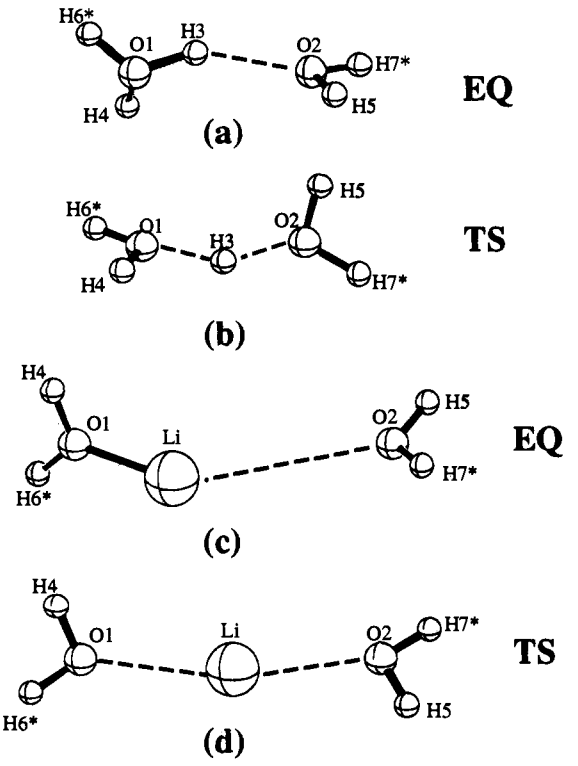

Figure 1. Equilibrium and transition state geometries of $(H_2O\cdot\cdot H\cdot\cdot OH_2)^+$ and $(H_2O\cdot\cdot Li\cdot\cdot OH_2)^+$, computed with external potential exerted on H* atoms.

Table 1. Equilibrium (EQ) and Transition State (TS) Geometries[a] of $(H_2O\text{-}H\text{-}OH_2)^+$ with the External Restraining Potential with k = 8 mdyn/Å and r_e = 4.5 Å

	EQ		TS	
geometric parameters[b]	SCF	MP2	SCF	MP2
	Bond Lengths (Å)			
O1O2	2.880	2.827	2.633	2.609
O1H3	0.983	1.010	1.322	1.312
O2H3	1.969	1.892	1.322	1.312
O1H4	0.958	0.976	0.953	0.972
O2H5	0.948	0.968	0.953	0.972
O1H6*	0.967	0.987	1.002	1.019
O2H7*	0.957	0.980	1.002	1.019
H6*H7*	4.487	4.485	4.447	4.453
	Bond Angles (deg)			
O1H3O2	153.09	152.63	169.67	167.96
O2O1H3	18.02	17.92	5.17	6.02
H4O1H6*	114.55	112.47	106.22	106.07
H5O2H7*	105.26	10.395	106.23	106.07
O2O1H4	101.50	101.42	105.58	105.48
O1O2H5	108.90	107.48	105.58	105.48
O2O1H6*	138.76	138.41	147.83	148.05
O1O2H7*	145.34	148.07	147.83	148.05
	Dihedral Angles (deg)			
H4O1O2H5	−118.67	−121.07	−127.18	−119.53
H6*O1O2H7*	−100.00	−96.19	−114.84	−138.00
H4O1O2H7*	57.08	48.39	43.99	51.24
H5O2O1H6*	90.25	94.35	43.98	51.24

[a] C_1 symmetry. [b] See Figure 1 for numbering of the atoms.

reduced R(OO). For example, the MP2 value of R(OO) decreases from 2.827 Å in the equilibrium structure to 2.609 Å in the transition state to proton transfer. Similar, albeit weaker, trends are witnessed in the lithium-bound complex where R(OO) shrinks from 5.942 to 5.806 Å and the Li bond becomes a few degrees closer to linearity. The intermolecular attraction also results in a reduction of the H*H* distance as compared to the r_e values of 4.5 and 7.5 Å for H^+ and Li^+, respectively. This

Table 2. Equilibrium (EQ) and Transition State (TS) Geometries[a] of $(H_2O\text{-}Li\text{-}OH_2)^+$ with the External Restraining Potential with k = 8 mdyn/Å and r_e = 7.5 Å

	EQ		TS	
geometric parameters[b]	SCF	MP2	SCF	MP2
	Bond Lengths (Å)			
O1O2	5.978	5.942	5.847	5.806
O1Li	1.885	1.922	2.933	2.910
O2Li	4.131	4.041	2.934	2.908
O1H4	0.949	0.968	0.947	0.967
O2H5	0.945	0.965	0.947	0.967
O1H6*	0.952	0.971	0.954	0.975
O2H7*	0.947	0.968	0.954	0.975
H6*H7*	7.496	7.496	7.489	7.489
	Bond Angles (deg)			
O1LiO2	166.10	169.72	170.54	172.58
O2O1Li	9.60	6.96	4.73	3.73
H4O1H6*	106.34	105.16	104.86	103.45
H5O2H7*	105.77	104.12	104.90	103.42
O2O1H4	114.73	117.22	108.94	110.76
O1O2H5	114.50	116.22	109.15	110.61
O2O1H6*	138.71	137.52	145.96	145.64
O1O2H7*	139.49	139.54	145.73	145.81
	Dihedral Angles (deg)			
H4O1O2H5	−114.38	−137.55	−113.94	−127.51
H6*O1O2H7*	−127.54	−146.82	−127.44	−139.20
H4O1O2H7*	58.89	37.57	59.35	46.61
H5O2O1H6*	59.18	38.06	59.24	46.68

[a] C_1 symmetry. [b] See Figure 1 for numbering of the atoms.

contraction amounts to about 0.05 Å in the former case but only about 0.01 Å for Li^+. The same force tends to elongate the O−H* bonds that involve the anchor hydrogens. Note also that the ϕ(H*OOH*) dihedral angle between the two anchor atoms is in the neighborhood of 100−140°. It appears in summary that the pivoting around the anchor hydrogens accounts for much more of the O··O contraction than any pulling together of the H* atoms against the external force.

Previous investigations[19] of H^+/Li^+ transfer in systems such as these have been limited to one of two extremes. In the case of adiabatic transfers, the ion is presumed to move sufficiently slowly that the remaining nuclei can adjust their relative positions at each stage of the transfer. As mentioned above, this treatment reveals the symmetric single well character of the PES of the isolated complex, with the bridging ion located squarely in the middle of the O··O axis, i.e. there is no real transfer. The other extreme "freezes" the interoxygen distance throughout the transfer process at some arbitrary value and permits free optimization of other geometrical parameters as the ion moves. The present prescription of a restraining force is free of the artificial restraint of the latter approach, yet it does keep the two oxygen atoms far enough apart to generate a proton transfer between two well-defined wells. It is thus possible to monitor the changes undergone by the complex as the proton is transferred. The contraction in the interoxygen separation is almost double in the case of H^+ transfer, compared to Li^+. The distance between the oxygens is shortened by inclusion of electron correlation and the equilibrium bond length from the proton donor O atom to H^+/Li^+ is reduced; all other bonds are lengthened. An important distinction between the two complexes is the distance that the central ion must move in order to reach the transition state. In $(H_2O\cdot\cdot H\cdot\cdot OH_2)^+$, the proton moves only about 0.3 Å from its equilibrium position to reach the top of the barrier, whereas Li^+ covers almost one full angstrom.

(19) (a) Scheiner, S. *J. Chem. Phys.* **1982**, *77*, 4039. (b) Scheiner, S. *J. Chem. Phys.* **1984**, *80*, 1982. (c) Hillenbrand, E. A.; Scheiner, S. *J. Am. Chem. Soc.* **1985**, *107*, 7690.

Table 3. Effect of Basis Sets on the Geometry of $(H_2O{-}H{-}OH_2)^+$ with No External Potential (with $k = 0$)

geometric parameters[a]	MP2/6-31+G**	MP2/6-311G (2df,p)[b]	MP2/6-311++G (2d,2p)[c]
	Bond Lengths (Å)		
O1O2	2.388		2.387
O1H3	1.194	1.193	1.195
O1H4	0.970	0.967	0.976
O1H6	0.970	0.967	0.976
	Bond Angles (deg)		
O1H3O2	174.6	174.6	174.1
H4O1H6	110.1	109.6	110.9
H4O1H3	118.7	119.4	
H6O1H3	119.4	117.3	
	Dihedral Angles (deg)		
H4O1H3O2	−158.9	−160.9	
H6O1H3O2	61.8	62.7	

[a] See Figure 1 for numbering of the atoms. [b] Reference 20. [c] Reference 14c.

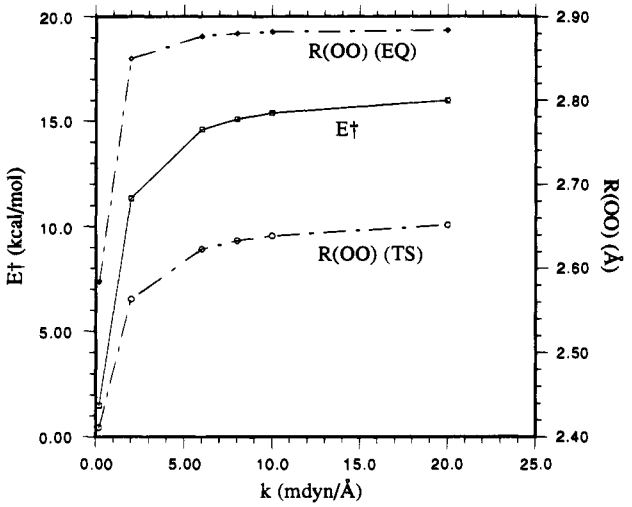

Figure 2. Variation of the proton transfer barrier, $E^\dagger$ (solid curve, left scale), and optimized R(OO) distances for $(H_2O\cdot\cdot H\cdot\cdot OH_2)^+$ (broken curves, right scale) with the force constant k in the external potential (see eq 1); $r_e = 4.5$ Å.

Extension of the basis set to triple-ζ quality (6-311+G**) with polarization functions on all the atoms plus a set of diffuse functions on oxygen has a negligible effect on the equilibrium (EQ) and transition state (TS) geometries of $(H_2O\cdot\cdot H\cdot\cdot OH_2)^+$. For example, the R(OO) distances are 2.883 and 2.637 Å in EQ and TS, respectively. The most extensive calculations on $(H_2O\cdot\cdot H\cdot\cdot OH_2)^+$ until now have been carried out by Janoschek[20] at the MP2 level using 6-311G(2df,p) and by Frisch et al.[14c] at the MP2/6-311++G(2d,2p) level. Table 3 compares the MP2/6-31+G** geometric parameters fully optimized (with no external potential) with the data accumulated earlier. There is little variation from one level of theory to the next; the proton lies halfway between the two oxygen atoms in all cases. It thus appears that 6-31+G** offers a well-balanced treatment of this system.

2. Tightness of the Spring. We next examine the consequences of differing degrees of flexibility in the protein backbone by varying the force constant, k in eq 1. The solid curve in Figure 2 illustrates the behavior of the proton transfer barrier height, $E^\dagger$, in $(H_2O\cdot\cdot H\cdot\cdot OH_2)^+$ as the "spring" becomes progressively more rigid. In the absence of any external potential ($k = 0$), $E^\dagger$ approaches zero (0.29 kcal/mol), which indicates the expected collapse of the transfer potential to a symmetric single well. This observation is consistent with the very short R(OO) distances, illustrated by the broken curves in Figure 2. As indicated by the right-hand scale in Figure 2, the equilibrium interoxygen distance is only about 2.4 Å. As the spring stiffens, it becomes more difficult for the intermolecular attraction to pull the two waters together so the interoxygen separation can no longer become so small. As a consequence, the proton transfer barrier climbs rapidly. After k has surpassed about 5−7 mdyn/Å, the barrier levels off and becomes less sensitive to further stiffening. This asymptotic behavior may be attributed to the fact that when the spring is sufficiently stiff, it effectively "tacks down" the two H* atoms, preventing the oxygens from approaching one another any more closely. Indeed, this expectation is confirmed by the similar asymptotic behavior of the R_{EQ} and R_{TS} curves in Figure 2. In the limit of very large k, the distance between the anchored H* atoms is fixed at 4.5 Å, and the barrier height is about 16.5 kcal/mol. It is important to note, however, that even with a fixed r(H*H*), the R(OO) distance is considerably smaller in the transition state than in the equilibrium geometry, enabled by a pivoting of each water molecule around the anchor hydrogen. It is interesting that the difference between R_{EQ} and R_{TS} remains almost constant, at 0.24 Å, over a wide range for larger values of k.

Table 4. Variation of Characteristics of Proton Transfer Profiles with Length of Spring with $k = 8$ mdyn/Å

	R(OO), Å		r(O1H3), Å		
r_e, Å	EQ	TS	EQ	TS	$E^\dagger$, kcal/mol[a]
4.5	2.827	2.609	1.010	1.312	8.6 (4.5)
4.2	2.585	2.481	1.048	1.244	1.2 (−2.0)
4.0	2.461	2.431	1.106	1.216	0.0

[a] Value in parentheses corrected by zero-point vibrational energy.

3. Length of the Spring. While the tightness of the spring reflects the rigidity with which the two subunits of the H bond are held in place, it is also of interest to examine the parametric dependence upon the length of the spring, i.e. how far apart the two subunits are held. This issue is of particular importance with respect to a recent suggestion that H bonds shorter than a minimal length can play a dramatic role in stabilizing interactions within proteins.[21]

Holding k equal to 8 mdyn/Å, r_e was set to three progressively shorter values of 4.5, 4.2, and 4.0 Å. Proton transfer potentials were computed at the correlated MP2 level for each pair of (k,r_e), again performing full optimization of the entire geometry at each stage of proton transfer. The resulting transfer profiles are summarized in Table 4 where it is indicated in the first row that a value of 4.5 Å for r_e yields a double-well potential, with a barrier height 8.6 kcal/mol. Contraction of the spring length by 0.3 Å reduces the barrier to 1.2 kcal/mol; the barrier vanishes entirely when the two anchor H* atoms are separated by 4.0 Å. Listed in parentheses in the final column are the barrier heights after zero-point vibrational energy has been included. The negative value for $r_e = 4.2$ Å indicates that the adiabatic barrier in fact vanishes for a spring length slightly greater than 4.2 Å.

Also reported in Table 4 are the optimized values of the H bond length, R(OO), and the bond length characterizing the bridging hydrogen in the equilibrium and transition state geometry. It may be noted that the 0.3 Å contraction of the spring length, from 4.5 to 4.2 Å, reduces the equilibrium R(OO) by 0.24 Å, but this quantity is lowered by only 0.13 Å in the transition state structure. The ensuing 0.2 Å reduction in r_e to 4.0 Å, which effectively removes the transfer barrier, reduces $R(OO)_{EQ}$ by 0.12 Å and $R(OO)_{TS}$ by only 0.05 Å. $R(OO)_{EQ}$

(20) Janoschek, R. *J. Mol. Struct. (THEOCHEM)* **1994**, *321*, 45.

(21) Cleland, W. W.; Kreevoy, M. M. *Science* **1994**, *264*, 1887−90. Frey, P. A.; Whitt, S. A.; Tobin, J. B. *Science* **1994**, *264*, 1927−30.

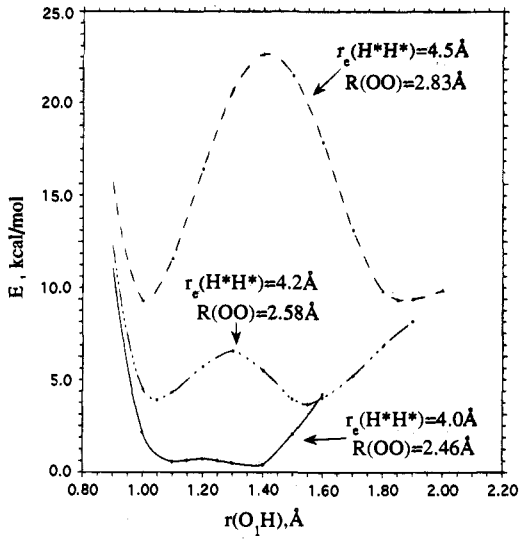

Figure 3. MP2 proton transfer potentials generated when R(OO) is held frozen at the values optimized for the equilibrium geometry.

and $R(OO)_{TS}$ differ by only a small amount for the very short H bond associated with $r_e = 4.0$ Å, with its very small barrier. The data reported for $r_e = 4.0$ Å in the last row of Table 4 are quite close to the potential obtained when the spring is removed entirely, in which case a full optimization of the complex yields R(OO) equal to 2.39 Å, with a symmetric single-well potential.

Figure 3 provides a clear illustration of the importance of permitting some vibrational freedom to the H bond length. The proton transfer potentials were generated by freezing the interoxygen distance to that value for which it is optimized with a given spring. So in the case of $r_e = 4.5$ Å, for example, R(OO) is optimized to 2.83 Å for the equilibrium geometry. When this distance is held fixed, the proton must surmount a barrier of some 14 kcal/mol, in contrast to the much smaller barrier of 8.6 kcal/mol when the interoxygen distance is permitted to fluctuate during the transfer. The barrier computed with R frozen for $r_e = 4.2$ Å is also somewhat higher than that obtained when the geometry is fully optimized at each stage of proton transfer.

4. Barrier Heights. The classical and adiabatic (zero-point corrected) barrier heights obtained at the SCF, MP2, MP3, and MP4SDTQ levels are listed in Table 5, using both the SCF and MP2 optimized geometries. In each case, the calculated barriers descend in the order SCF > MP3 > MP4SDTQ > MP2, consistent with earlier studies.[7] The barriers are stable with respect to basis set enlargement: The SCF proton transfer barrier of $(H_2O\cdot\cdot H\cdot\cdot OH_2)^+$ increases by only 0.19 kcal/mol with the extension from 6-31+G** to 6-311+G**. Our estimate at the MP4SDTQ/6-31+G**//MP2/6-31+G** level, with MP2/6-31+G** zero-point correction, is some 5.3 kcal/mol. The corresponding Li^+ transfer barrier is slightly higher at 7.1 kcal/mol. Indeed, Table 5 indicates that the barrier for Li ion transfer is consistently higher than that of the proton transfer. This result should not be taken as a general physical principle since it is influenced by the external potential which helps determine the intermolecular separation.

5. Intrinsic Reaction Coordinate Analysis. Figure 4 displays the potential energy profiles for transfer in $(H_2O\cdot\cdot H\cdot\cdot OH_2)^+$ and $(H_2O\cdot\cdot Li\cdot\cdot OH_2)^+$ along the intrinsic reaction coordinate, calculated at the SCF level. It is apparent at first glance that the proton transfer process in Figure 4a is "sharper", i.e. the barrier is narrower, than in the case of Li^+. The width at half-height is less than 1 $amu^{1/2}$ bohr in the former case and six times that in the latter. There is also more of a

Table 5. Energy Barrier (kcal/mol) for Proton and Lithium Ion Transfer with External Restraining Potential with $k = 8$ mdyn/Å, $r_e = 4.5$ and 7.5 Å

	classical barrier height	zero-point correction	vib adiabatic barrier height
	H^+ Transfer Barrier		
	SCF Geometry (6-31+G**)		
SCF	15.09	−3.96	11.13
MP2	8.08		4.12
MP3	10.01		6.05
MP4SDTQ	8.88		4.92
	MP2/6-31+G** Geometry		
SCF	14.49		10.43
MP2	8.60	−4.06	4.54
MP3	10.34		6.28
MP4SDTQ	9.40		5.34
	Li^+ Transfer Barrier		
	SCF Geometry (6-31+G**)		
SCF	9.23	−0.71	8.52
MP2	7.71		7.00
MP3	8.19		7.48
MP4SDTQ	7.77		7.06
	MP2/6-31+G** Geometry		
SCF	9.21		8.49
MP2	7.72	−0.72	7.00
MP3	8.20		7.48
MP4SDTQ	7.77		7.05

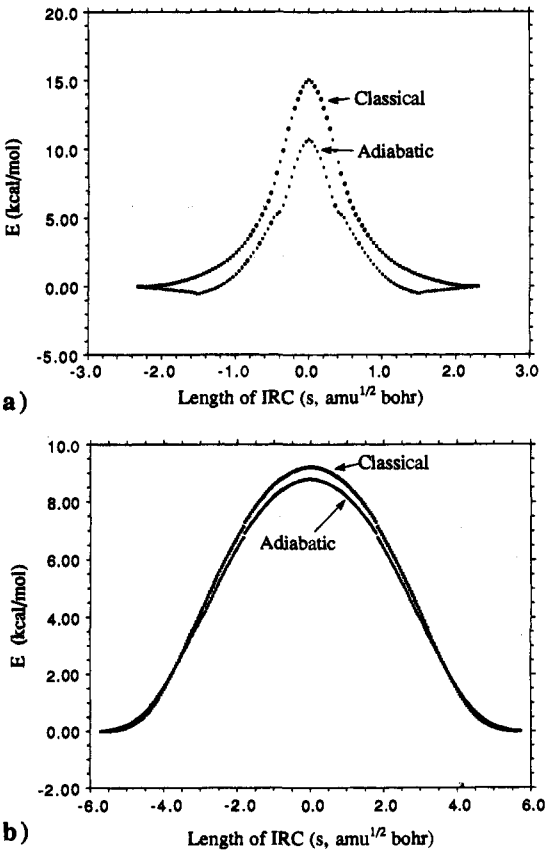

Figure 4. Potential energy profiles for proton transfer along the intrinsic reaction coordinate s in (a) $(H_2O\cdot\cdot H\cdot\cdot OH_2)^+$ and (b) $(H_2O\cdot\cdot Li\cdot\cdot OH_2)^+$. In each case, the upper curve represents the purely classical energy and the lower refers to the vibrationally adiabatic profile.

separation between the classical and adiabatic energies in the proton transfer, indicating a greater effect of vibrational energies. Note also the small dip in adiabatic energy, below zero, on either side of the barrier, which results from the lowering in vibrational energy.

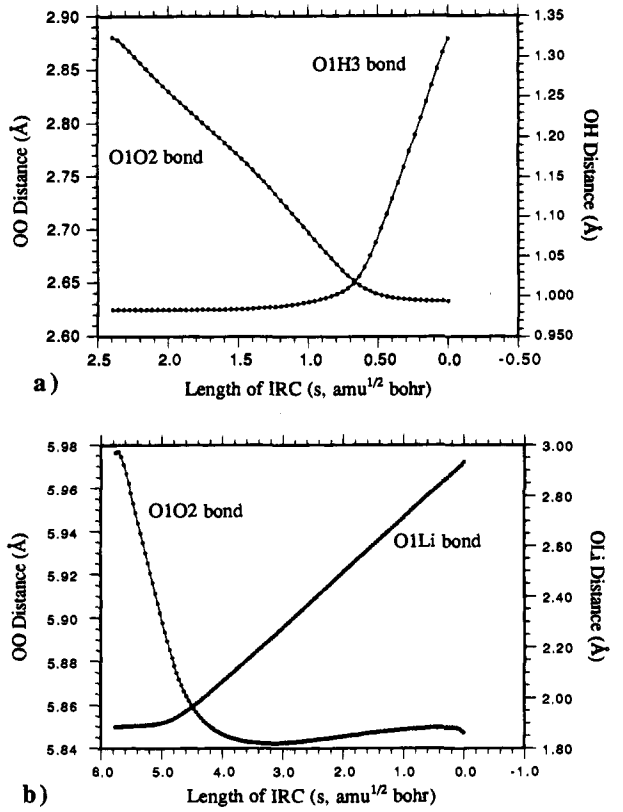

Figure 5. Variation of interatomic distances along the intrinsic reaction coordinate s of (a) $(H_2O\cdot\cdot H\cdot\cdot OH_2)^+$ and (b) $(H_2O\cdot\cdot Li\cdot\cdot OH_2)^+$.

The minimum energy path (MEP) on the potential energy surface for the proton transfer from one water molecule to another involves a complex set of nuclear displacements. Comparison of the geometric parameters at the equilibrium and transition states in Table 1 reveals that, besides the contraction of the OO distance and stretching of the O1−H bond, some of the bond and dihedral angles change significantly, corresponding to reorientation of the OH_2 molecules. The variation of the OO and O1H3 distances as a function of the IRC is illustrated in Figure 5a, from which it may be noted that the proton transfer process seems to be a composite of two nearly separate steps. Starting at the equilibrium geometry on the left side of Figure 5a ($s \sim 2.4$), the initial motion along the MEP is predominantly heavy atom displacement (step 1), bringing the two oxygen atoms closer to each other. As the path approaches the barrier and s diminishes to about 0.7, the O−O contraction ceases and the remainder of the path involves chiefly hydrogenic motion as the proton is transferred (step 2). A similar two-step reaction path has been observed in the proton transfer in formic acid dimer[22] and in $C_2H_7^-$.[23]

As pointed out above, the H bond is significantly more linear in the transition state than equilibrium geometry. For example, the MP2 value of the θ(O2O1H3) angle shrinks from 18° to 6°. Monitoring of the IRC indicates that, beginning with the equilibrium geometry, the intermolecular angle first becomes more nonlinear, before starting to change toward linearity. Most of this change occurs in the first step ($s > 0.65$) where the O atoms approach one another, in step 2 ($s < 0.65$) where the proton transfer *per se* is actually occurring, the angle remains constant. From the energetic point of view, the approach of the OH_2 fragments in step 1 accounts for an energy increase of about 5.0 kcal/mol, 30% of the full barrier height.

(22) Shida, N.; Barbara, P. F.; Almlöf, J. *J. Chem. Phys.* **1991**, *94*, 3633.
(23) Isaacson, A. D.; Wang, L.; Scheiner, S. *J. Phys. Chem.* **1993**, *97*, 1765.

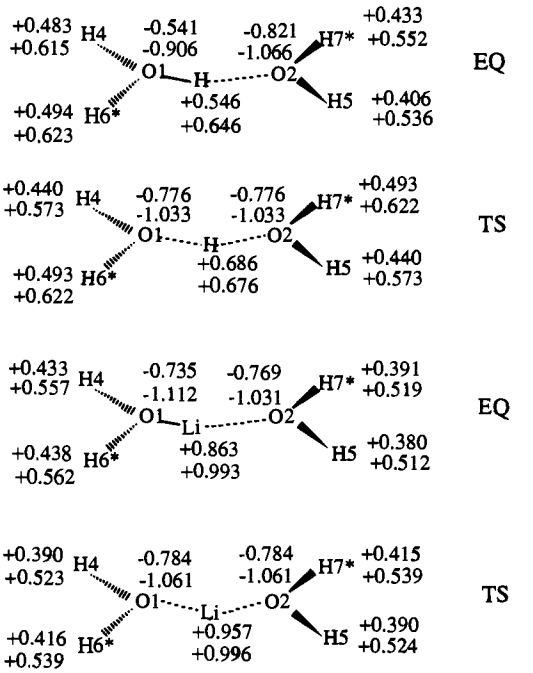

Figure 6. Mulliken (upper) and natural (lower) atomic charges. EQ and TS designations refer to equilibrium and transition state geometries for $k = 8$ mdyn/Å and $r_e = 4.5$ (H) and 7.5 Å (Li^+).

There are some interesting comparisons with the lithium ion transfer pictured in Figure 5b. Like the process in $(H_2O\cdot\cdot H\cdot\cdot OH_2)^+$, there are clearly two different steps in the process. The first step is largely approach of the two O atoms, followed thereafter by the displacement of the central ion. An important point of departure from the proton case is in the timing of the two steps. The O··O contraction is largely completed by the time that s has decreased to about 4.5, after which this distance is relatively constant. It does undergo a very minor stretch near the TS, but this amounts to less than 0.01 Å. As s diminishes below 5, the Li begins to move away from O1 and continues this motion until the transition state has been reached. This ion moves a total of about 1.0 Å from its equilibrium position to the transition state, almost three times more than the motion of H^+. Most of the increased linearity of the O−Li−O angle takes place in the first step, which covers only 10% of the full energy rise.

6. Electron Density Rearrangements. The proton transfer from one molecule to another in a H-bonded complex is accompanied by transfer of electron density in the opposite direction[24] and redistributions within each subunit. The recent monitoring of individual atomic charges by Florian and Scheiner[25] was limited in the sense that the interoxygen distance was kept fixed during the transfer process, as were certain other features of the geometries. No attempt was made to identify or follow a minimum energy path along the surface. In the present investigation we have computed atomic charges using both Mulliken (MPA)[26] and natural population analysis (NPA)[27] schemes at the SCF level.

The charges at the equilibrium and transition state geometries of the H^+ and Li^+ transfers are reported in Figure 6. Differences between these quantities are indicative of electronic rearrangements that accompany motion of the proton from its equilibrium position to a location halfway between the two O atoms.

(24) Scheiner, S. *J. Chem. Phys.* **1981**, *75*, 5791.
(25) Florian, J.; Scheiner, S. *J. Comp. Chem.* **1994**, *15*, 553.
(26) Mulliken, R. S. *J. Chem. Phys.* **1955**, *23*, 1833.
(27) Reed, A. E.; Weinstock, R. B.; Weinhold, F. *J. Chem. Phys.* **1985**, *83*, 735.

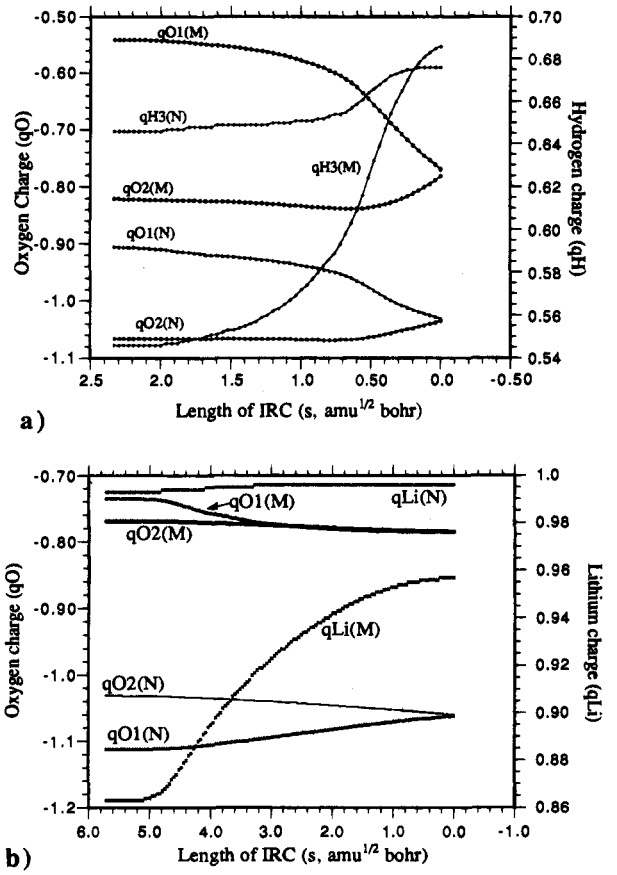

Figure 7. Variation of atomic charges in (a) $(H_2O\cdot\cdot H\cdot\cdot OH_2)^+$ and (b) $(H_2O\cdot\cdot Li\cdot\cdot OH_2)^+$ as the intrinsic reaction coordinate s progresses. M and N refer to Mulliken and natural charges, respectively.

Consistent with prior findings, the half-transfer of the proton leads to increased electron density on the proton donor, with most of it accumulating on the oxygen atom. Most of this density originates on the acceptor molecule, with a significant amount derived from the transferring hydrogen which becomes more positively charged. Although the magnitudes of the natural charges are higher (more ionic) than the Mulliken charges, the changes accompanying half proton transfer are remarkably similar and the amount of charge transferred from the proton acceptor molecule is the same in either framework (0.14 e). It is interesting also that the starred "anchor" hydrogens are more positively charged than their counterparts on the same molecule.

Similar trends are observed in the Li^+ transfer although there are certain differences. Instead of losing electron density, the acceptor atom O2 becomes slightly more negative as the lithium approaches. The Mulliken charge of the central Li grows by about 0.1 e as a result of its half-transfer, whereas the NPA charge is virtually unchanged. Only a very small amount of electron density is lost from the Li^+ acceptor molecule. In either case, the charge assigned to the Li center is considerably larger than that of the central proton.

Now let us turn our attention to the variation of atomic charges as the reaction follows along the intrinsic reaction coordinate s, illustrated in Figure 7. Note that the scale used for the negatively charged O atoms is on the left of Figure 7, and the positive hydrogen charges are measured by the right scale. Consistent with the two separate stages of the reaction as marked by geometric changes, the initial stages of the reaction cause only small perturbations in the charges of the various atoms. It is only after the second step has been entered, i.e. when the central ion is undergoing the bulk of its motion, that the charges begin to change significantly. These changes are uniform along the IRC, and largely monotonic.

4. Conclusions

Imposition of an external force between hydrogen atoms of each water molecule successfully keeps the two oxygen atoms far enough apart to generate a true double-minimum transfer potential, without recourse to artificially fixing R(OO) to a constant value. It is then possible to locate the positions of the minima and the cation transfer transition state and to study the intrinsic reaction coordinate that connects them. The proton and lithium ion transfer paths have much in common. There are clearly two separate steps: The ion undergoes little motion until the two O atoms have approached one another. The bulk of the electronic redistribution is delayed until the central ion is actually moving.

There are some interesting differences observed between the Li^+ and H^+ transfer cases. The Li^+ moves about 1.0 Å during its half-transfer, as compared to a displacement of only 0.3 Å for the proton. Yet the contraction of the $R(O\cdot\cdot O)$ distance upon half transfer is twice as large for proton transfer, compared to Li^+. Also, the proton transfer barrier is only about one-sixth as wide as the energy hill facing Li^+.

Along with the stretching of the O··O distance that is a natural consequence of the external force, the attraction between the two oxygen atoms induces a pivoting of each water molecule about its anchor hydrogen that in turn results in a nonlinear H or Li bond. As the force constant connected with the external spring is increased, and the two water molecules are held more rigidly apart, the energy barrier to transfer increases up to a limiting value. Also displaying asymptotic behavior is the amount that R(OO) contracts upon half transfer, which reaches 0.24 Å in the case of H^+. Shortening of the spring reduces the barrier to proton transfer, whether or not R(OO) is held frozen or permitted to adjust as the proton is being displaced. On the other hand, allowing the two subunits to oscillate freely during the transfer process leads to a shortened H bond at the transfer midpoint and a significantly lower energy barrier.

An approach such as the one considered here, where a spring of adjustable length and stiffness is inserted between a pair of atoms, one of each subunit, provides a framework by which to study in a systematic manner how the structural elements of a given macromolecule can influence the cation transfer process. The adjustable nature of the external force makes the approach considerably more flexible than performing calculations upon a large molecule, incorporating an intramolecular H bond. In such a case, the geometry of the H bond is determined by the structural restraints of the particular molecule considered, making systematic variation difficult, and at times erratic. For example, the R(NN) distance in the cyclic intramolecular H bond of $NH_2(CH_2)_nNH_3^+$ does not vary smoothly with n, increasing from 2.44 Å for $n = 3$ to 2.64 and 2.69 Å for $n = 4$ and 5, respectively.[28] In contrast, the H bond in malonaldehyde $OH(CH)_3O$[29] has the two oxygen atoms separated by some 2.6 Å, but this distance is shortened to 2.46 Å when the number of intervening C atoms is increased by 1.[30]

In addition to providing the capacity for systematic variation in H bond geometries, incorporation of an external force has an additional advantage over the quantum mechanical calculation

(28) Duan, X.; Sheiner, S. *J. Am. Chem. Soc.* **1992**, *114*, 5849.
(29) Frisch, M. J.; Scheiner, A. C.; Schaefer, H. F., III; Binkley, J. S. *J. Chem. Phys.* **1985**, *82*, 4194. Shida, N.; Barbara, P. F.; Almlöf, J. E. *J. Chem. Phys.* **1989**, *91*, 4061. Luth, K.; Scheiner, S. *J. Phys. Chem.* **1994**, *98*, 3582.
(30) George, P.; Bock, C. W.; Trachtman, M. *J. Phys. Chem.* **1983**, *87*, 1839.

of a larger system. The accuracy with which a calculation may be carried out, i.e. the size of the basis set or level of correlation, drops quickly as the number of electrons that must be explicitly considered rises. The study of a ring system containing an intramolecular H bond, like malonaldehyde, necessitates a computation of all electrons of the atoms of the ring, in addition to the pertinent atoms of the H bond itself. In contrast, using an external force adds no further electrons to the system, permitting a high level of theory to be applied.

Acknowledgment. We gratefully acknowledge useful discussions with Prof. A. Isaacson and Dr. J. Florian and support of this work by the National Institutes of Health (GM29391).

JA942548+